Modeling Salt Water Intrusion in Tanshui River Estuarine System—Case-Study Contrasting Now and Then

Wen-Cheng Liu[1]; Ming-Hsi Hsu[2]; Chi-Ray Wu[3]; Chi-Fang Wang[4]; and Albert Y. Kuo, M.ASCE[5]

Abstract: A vertical (laterally integrated) two-dimensional numerical model was applied to study the salt water intrusion in the Tanshui River estuarine system, Taiwan. The river system has experienced dramatic changes in the past half century because of human intervention. The construction of two reservoirs and water diversion in the upper reaches of the river system significantly reduces the freshwater inflow. The land subsidence within the Taipei basin and the enlargement of the river constriction at Kuan-Du have lowered the river bed. Both changes have contributed farther to the intrusion of tidal flow and salt water in the upstream direction. The model was reverified with the earliest available hydrographic data measured in 1977. The overall performance of the model is in reasonable agreement with the field data. The model was then used to investigate the change in salt water intrusion as a result of reservoir construction and bathymetric changes in the river system. The model simulation study reveals that significant salinity increases have resulted from the combined changes. It has been speculated by ecological researchers that the long-term increase in salinity might be the driving force altering the aquatic ecosystem structure in the lower reach of the estuary and the Kuan-Du mangrove swamp, particularly the enlargement of the mangrove area and the disappearance of freshwater marshes. However, concrete proof has not been available since no prototype salinity data were available prior to the reservoir construction. This case study offers the first quantitative estimate of the salinity changes due to human interference in this natural system.

DOI: 10.1061/(ASCE)0733-9429(2004)130:9(849)

CE Database subject headings: Salt water intrusion; Taiwan; River systems; Numerical models; Reservoirs; Bathymetry.

Introduction

Throughout the history of civilization, mankind has tended to concentrate its activities along the courses of rivers. This has naturally led to the imposition of man-made changes on rivers, through the construction and operation of dams and reservoirs, river training and dredging, waste disposal, etc. An increasing number of diverse projects have required modifications to river systems, such as reservoir regulation or freshwater withdrawals. In these cases, upstream changes of the river runoff will inevitably have consequences on the estuarine portion of the river. Although river management has commonly occurred over the past 50 years, most studies have focused on the short or medium term behavior of estuarine flows, few studies have been conducted and little is known about the long-term estuarine response associated with river management schemes (Kjerve 1976; Kjerfve and Greer 1978; McAlice and Jaeger 1983). For these reasons, there is a need for numerical modeling in conjunction with any estuary-related management plans. Numerical models have become important tools to assess the response of natural systems to changes in environmental regulations and construction of engineering facilities.

The Tanshui River estuary (Fig. 1) is the largest estuarine system in Taiwan, with its drainage basin including the capital city of Taipei. The tidal influence spans a total length of about 82 km, encompassing the entire length of the Tanshui River and the downstream reaches of its three major tributaries: the Tahan Stream, the Hsintien Stream, and the Keelung River. Except during the period of a flood event, the astronomical tide may reach as far upriver as Cheng-Ling Bridge in Tahan Stream, the Hsiu-Lang Bridge in Hsintien Stream, and the Chiang-Pei Bridge in Keelung River (Fig. 1). Tidal propagation is the dominant mechanism controlling the water surface elevation, and ebb and flood flows. The M_2 tide is the primary tidal constituent at the river mouth, with a tidal range of 2.17 m at mean tide, and up to 3 m at spring tide. Because of the cross-sectional contraction and wave reflection, the mean tidal range may reach a maximum of 2.39 m within the system. The phase relationship between tidal elevation and tidal flow is close to standing wave characteristics (Hsu et al. 1999a).

Sea water intrudes upriver as a result of tidal advection and the classical two-layer estuarine circulation. Salinity varies in intratidal time scale in response to the ebb and flood of the flows as well as in various longer time scales in response to freshwater inflow. The limit of salt intrusion may reach beyond 25 km in the Tahan Stream from the river mouth during the period of low flow.

[1]Associate Professor, Dept. of Civil Engineering, National United Univ., Miao-Li 360, Taiwan. E-mail: wcliu@hy.ntu.edu.tw

[2]Professor, Dept. of Bioenvironmental Systems Engineering and Senior Research Fellow, Hydrotech Research Institute, National Taiwan Univ., Taipei 10617, Taiwan (corresponding author) E-mail: mhhsu@ccms.ntu.edu.tw

[3]Doctoral Student, Dept. of Bioenvironmental Systems Engineering, National Taiwan Univ., Taipei 10617, Taiwan.

[4]Doctoral Student, Dept. of Bioenvironmental Systems Engineering, National Taiwan Univ., Taipei 10617, Taiwan.

[5]Visiting Professor, Dept. of Bioenvironmental Systems Engineering and Senior Research Fellow, Hydrotech Research Institute, National Taiwan Univ., Taipei 10617, Taiwan.

Note. Discussion open until February 1, 2005. Separate discussions must be submitted for individual papers. To extend the closing date by one month, a written request must be filed with the ASCE Managing Editor. The manuscript for this paper was submitted for review and possible publication on November 25, 2002; approved on February 10, 2004. This paper is part of the ***Journal of Hydraulic Engineering***, Vol. 130, No. 9, September 1, 2004. ©ASCE, ISSN 0733-9429/2004/9-849–859/$18.00.

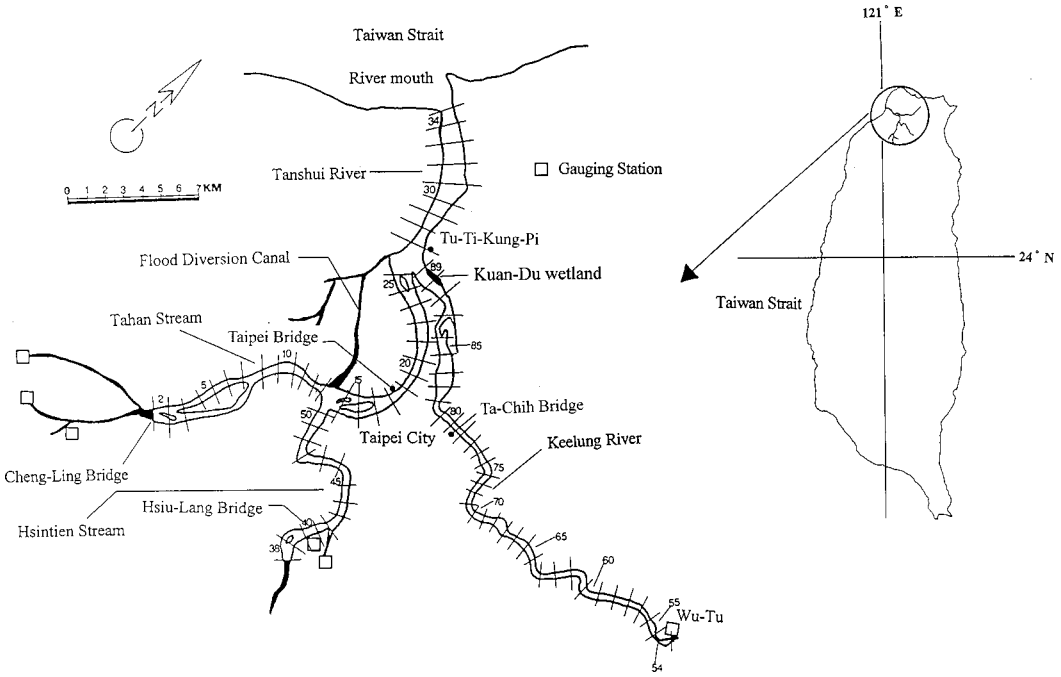

Fig. 1. Map of Tanshui River system and model segments

The baroclinic pressure gradient set up by the salinity distribution is large enough to push the denser salt water upriver along the bottom layer of the estuary. This results in the classical two-layer circulation of net upriver flow in the bottom layer and net downriver flow in the upper layer (Hsu et al. 1999a). The resulting estuarine circulation strengthens as the river flow decreases (Kuo and Liu 2001).

Two reservoirs, Feitsui Reservoir and Shihman Reservoir, were built in the upriver reaches of the Tanshui River system. Feitsui Reservoir, completed in 1987, had an initial design capacity of 406×10^6 m^3 and was primarily designed to provide domestic water supply to the Taipei metropolitan area with a population over 5 million. The dam site of the Feitsui Reservoir is located at the lower end of the Peishih Stream, a tributary of the Hsintien Stream, and is about 30 km away from Taipei City. Shihmen Reservoir was completed in 1964 and situated at the upper end of the Tahan Stream. This multipurpose reservoir supplies water to the rice fields of northwest Taiwan and to Taipei during the dry season. Covering 8 km^2, this man-made reservoir also generates 87,400 kW of electricity for the island's insatiable demand. Another vital function of these two reservoirs is to provide flood control in the typhoon season. Fig. 2(a) presents flow duration curves in the Tahan Stream before and after the Shihman Reservoir construction. Fig. 2(b) shows flow duration curves in the Hsintien Stream before and after the Feitsui Reservoir construction. These figures indicate that the river discharges have dramatically reduced after the reservoirs were constructed. As an example, the current Q_{50} flow is 50% less than that before the Shihman Reservoir construction.

The Taiwan Water Resources Agency has conducted regular bathymetric surveys of the river system since 1969. It measured the cross-sectional profiles of the river at about 0.5 km intervals along the tidal portion of the river. The survey results show considerable bathymetric change in the estuarine system. Fig. 3 compares the 1995, 1977, and 1969 river bed profiles, plotted along the river axis in the Tanshui River-Tahan Stream and Hsintien Stream. It shows that there has been extensive scouring along

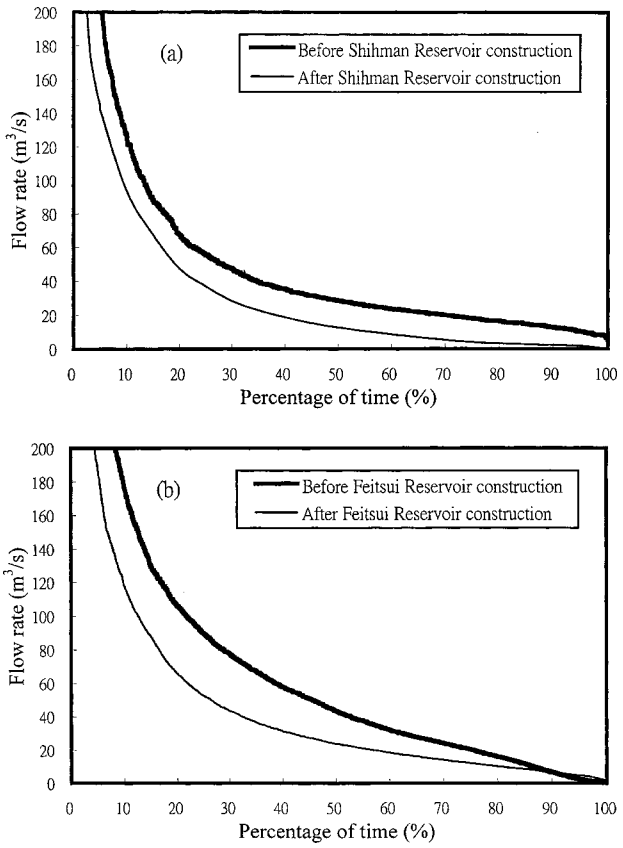

Fig. 2. Comparison of flow duration curves before and after reservoir construction in the (a) Tahan Stream and (b) Hsintien Stream

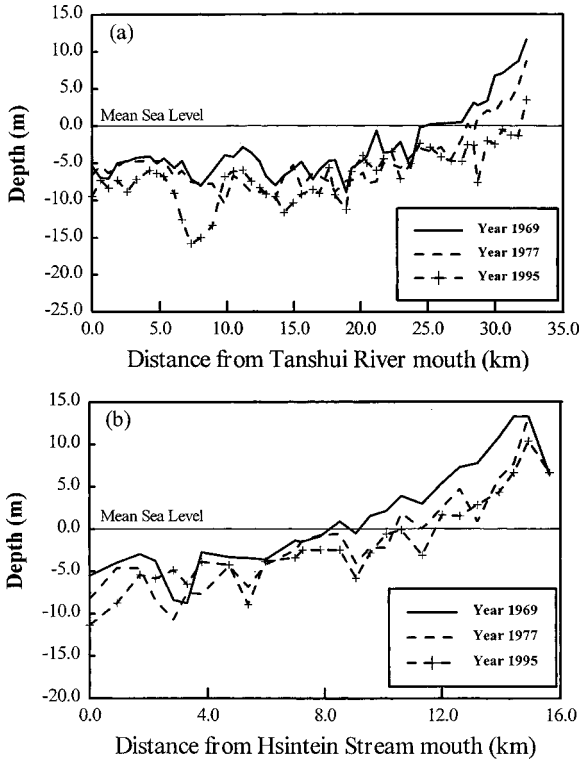

Fig. 3. Comparison of 1995, 1977, and 1969 bottom profiles: (a) Tanshui River—Tahan Stream and (b) Hsintien Stream

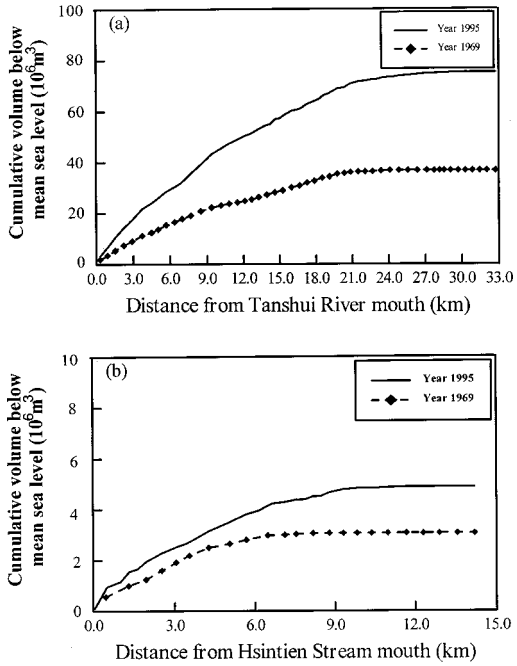

Fig. 4. Comparison of 1995 and 1969 cumulative volume below mean sea level: (a) Tanshui River—Tahan Stream and (b) Hsintien Stream

most of the river system, except for some local reaches. This results in a substantial increase in the cumulative volume below mean sea level for the entire estuarine system (Fig. 4).

Kuan-Du wetland is the largest estuarine wetland in the Tanshui River system. It is situated on the northern shore of the Keelung River mouth (Fig. 1). It was reported that the vegetation types in the wetland had shifted from less salt-tolerant types to salt-tolerant types, namely mangroves. Using geographic information system and image processing techniques, Wang (1999) interpreted a series of aerial photos from 1978 to 1997 to delineate the area extent of the three dominant types of vegetation in the wetland. He reported that the mangrove *Kandelia candel* had increased its aerial coverage from nearly 0 to 24 ha, about 68% of the total area. The less salt-tolerant *Cyperus malaccensis* decreased from 10 ha in 1978 to none in 1997, while *Phragmites communis* decreased from about 20 to 10 ha. Wester (1988) suggested that the salinity increase in the river waters adjacent to the wetland might be the most important factor responsible for the continuing shift in vegetation type. Land subsidence was cited as the major culprit. It is expected that either of the two alternations of the river system described above will enhance the salt water intrusion into the system.

In this study, a vertical (laterally integrated) two-dimensional hydrodynamic model was applied to study the Tanshui River estuarine system. The model had previously been calibrated and verified for the recent conditions of 1994 and 1995 (Hsu et al. 1999a). The model was further reverified with the earliest available prototype data of 1977. The verified model was then used to simulate salt water intrusion under both the current conditions and the prereservoir conditions, respectively. The results show that the increase in salt water intrusion has the potential to favor the development of mangrove wetlands in the lower estuary near Kuan-Du.

Model Description

Many numerical models have been developed to simulate the hydrodynamic behavior of estuaries using one-, two-, or three-dimensional frameworks. Although full three-dimensional models (e.g., Casulli and Cheng 1992; Johnson et al. 1993; Wang et al. 1994; Blumberg et al. 1999; Lai et al. 2003) have increasingly been used, a two-dimensional laterally integrated model offers an efficient and practical tool for narrow and partially mixed estuaries. In a narrow channel with steep bathymetric variations, a sufficiently fine grid must be designed for a three-dimensional model to resolve the lateral bathymetric gradients. It is computationally intensive and often unnecessary since the dominant transport mechanisms and their variations are in the longitudinal and vertical directions.

A laterally integrated two-dimensional, real-time model of hydrodynamics and salinity was developed for application to the tidal portion of the Tanshui River estuarine system (Hsu et al. 1996, 1997). The model is actually quasi-three-dimensional, since it also includes the simulation of shoals and shallow embayments adjacent to the main channel. It simulates the shallow areas as temporary storages which communicate with the channel as the tide rises and falls (Park and Kuo 1995). The model is based on the principles of conservation of mass, momentum, and solute mass.

Basic Equations

In a right-handed Cartesian coordinate system, with the x axis directed seaward and the z axis directed upwards, the equations for the hydrodynamic model are as follows:

laterally integrated continuity equation

$$\frac{\partial(uB)}{\partial x}+\frac{\partial(wB)}{\partial z}=q_p \tag{1}$$

laterally integrated momentum equation

$$\frac{\partial(uB)}{\partial t}+\frac{\partial(uBu)}{\partial x}+\frac{\partial(uBw)}{\partial z}=-\frac{B}{\rho}\frac{\partial p}{\partial x}+\frac{\partial}{\partial x}\left(A_xB\frac{\partial u}{\partial x}\right)+\frac{\partial}{\partial z}\left(A_zB\frac{\partial u}{\partial z}\right) \quad (2)$$

hydrostatic equation

$$\frac{\partial p}{\partial x}=\rho g\frac{\partial \eta}{\partial x}+g\int_z^{\eta}\frac{\partial \rho}{\partial x}dz \quad (3)$$

sectionally integrated continuity equation

$$\frac{\partial}{\partial t}(B_\eta \eta)+\frac{\partial}{\partial x}\int_{-H}^{\eta}(uB)dz=q \quad (4)$$

laterally integrated mass balance equation for salt

$$\frac{\partial(sB)}{\partial t}+\frac{\partial(sBu)}{\partial x}+\frac{\partial(sBw)}{\partial z}=\frac{\partial}{\partial x}\left(K_xB\frac{\partial s}{\partial x}\right)+\frac{\partial}{\partial z}\left(K_zB\frac{\partial s}{\partial z}\right)+S_0 \quad (5)$$

equation of state

$$\rho=\rho_0(1+ks) \quad (6)$$

where x=distance seaward along the river axis; z=distance upward in the vertical direction; t=time; q_p=lateral inflow per unit lateral area; q=lateral inflow per unit river length; η=position of the water surface above mean sea level; s=laterally averaged salinity; u and w=laterally averaged velocity components in the x and z directions, respectively; B=river width; B_η=width at the water surface including side storage area; H=total depth below the mean sea level; p=pressure; g=gravitational acceleration; A_Z and K_Z=turbulent viscosity and diffusivity, respectively, in the z direction; A_x and K_x=dispersion coefficients for momentum and mass, respectively, in the x direction; ρ and ρ_0=water density and freshwater density, respectively; k=constant relating density to salinity ($=7.5\times10^{-4}$/ppt); and S_0=source and sink of salt due to exchange with side storage area.

Boundary Conditions

To seek upstream boundary conditions not influenced by the tide, the computational domain of a model should be extended to, or beyond, the tidal limits in the tributaries as well as in the mainstem. For tidal rivers with a well-defined fall line, the tidal limits are located at fixed points. They are ideal locations as the upstream boundaries of the model domain. The boundary condition there may be specified with a freshwater discharge as mass input without contribution to momentum. For tidal rivers with a bottom elevation rising gradually above mean sea level, the tidal limits move up or down the rivers in response to the decrease or increase of river discharges. The model limit should be at a location where the bottom elevation is higher than high tide level. The river discharge should contribute both the mass and momentum at this type of upstream boundary. The Tanshui River system is of the second type of boundary condition. The upstream boundaries of the model domain are located upriver of the tidal limits in all three tributaries. The daily freshwater discharges are specified and the salinity is assumed to be zero at these boundaries.

The downstream boundary is located at the river mouth where the water surface elevation and high tide salinity are specified. The water surface elevation may be input as a time series of prototype data or the amplitudes and phases of tidal constituents. The specified salinity is the ''ocean'' salinity which is assumed to exist off the mouth of the estuary. During flood tide, the ocean water is advected into the estuary, increasing the salinity at the mouth, the model's downstream boundary, until the ocean salinity is reached. A period of adjustment is allowed after the flow starts to flood and before the salinity at the mouth reaches the specified ocean salinity. In this model, an input parameter is assigned for the specification of this adjustment period, and the salinity is assumed to increase linearly with time during this period. Therefore the specified ocean salinity is the salinity for only a portion of the incoming tide. The adjustment period may be determined through prototype data analysis and model calibration. During ebb tide, the longitudinal salinity profile is assumed to have advected out of the mouth as a ''frozen'' pattern, i.e., neglecting diffusion.

Numerical Methods

The system of equations is solved using the finite difference method with a uniform grid of spatially staggered variables. The staggered grid structure, also used in many other models, permits easy application of boundary conditions and evaluation of the dominant pressure gradient force without interpolation or averaging (Blumberg 1977). Since the vertical two-dimensional hydrodynamic model does not include the Coriolis term, a two-time level scheme is used to approximate the time derivative terms in the equations. This avoids the problem of time-step splitting which is often associated with a three-time level scheme.

Large vertical gradients of variables (u and s) require a grid size that is much smaller in the vertical direction than in the horizontal direction. To accomplish this, the fluid motion is considered in horizontal slices with an exchange of momentum and mass between these slices. Integration over the height of the layer is performed assuming that all variables are practically constant through the depth of each layer. Eqs. (1), (2), and (5) are integrated over a layer of finite thickness and then solved with Eqs. (3), (4), and (6). The implicit treatment of the vertical diffusion terms results in a tridiagonal matrix in the vertical direction, which is solved using a *LINPACK* subroutine developed at the Argonne National Laboratory. To improve numerical stability, the pressure gradient term in Eq. (3) is evaluated using η at the new time step. All other terms are evaluated explicitly.

In the numerical treatment of the advection term, central and upwind (or upwind weighted) differences are the two routinely used schemes. Though the central difference scheme is second-order in accuracy and free of numerical diffusion, it is nonconvergent, particularly in regions where advection dominates over diffusion (Roache 1972). The unstable feature of a central difference scheme becomes more problematic in the mass balance equation [Eq. (5)] than in the momentum equation [Eq. (2)] in which the sink term (friction) tends to dissipate this oscillatory behavior. Primary dynamic balance in partially mixed estuaries is between the surface slope, density gradient, and vertical gradient of turbulent shear stress (Pritchard 1956). Since the horizontal and vertical advection terms are not important in the momentum equation, they are approximated with the central difference scheme.

The dominant salt balance, however, takes place between horizontal advection and vertical turbulent diffusion (Pritchard 1954), making the accurate numerical treatment of horizontal advection essential to the model behavior. While the relatively small vertical advection term can be treated with the central difference scheme, the horizontal advective transport should be modeled with minimal introduction of artificial numerical oscillation or diffusion.

The QUICKEST (quadratic upstream interpolation for convective kinematics with estimated streaming terms) scheme, which has been successfully applied to the modeling of an advection term (Leonard et al. 1978; Hall and Chapman 1985; Johnson et al. 1993), is used for the Tanshui River modeling.

Vertical Turbulent Diffusion Coefficients

The system of equations may be closed with the parameterization of Reynolds stress and turbulence flux terms. Formulation of the Reynolds stress and flux terms mathematically, i.e., the turbulent closure model, has been, and still is, one of the most problematic steps for the laterally integrated two-dimensional or three-dimensional numerical models. The current practice ranges from a simple eddy viscosity approach to more complicated second order closure schemes (Blumberg 1986). The most reasonable way, with the current understanding of the turbulent mixing processes, is to choose cautiously the best method for an application and to calibrate it by comparison with field data (Wang et al. 1990). The oldest, yet still the most popular method of parameterizing the Reynolds terms, is the one based upon the eddy viscosity hypothesis. In Eqs. (2) and (5), the Reynolds terms are already expressed in terms of eddy viscosities and diffusivities.

It has long been found that the vertical mixing of mass and momentum are, in some sense, formally linked with water column stability through a quantity such as the gradient Richardson number. Through theoretical arguments or empirical deductions, a number of functional relationships between the vertical diffusion coefficients of mass, K_Z, and momentum, A_Z, have been proposed. For flow with two parallel plane boundaries in a wide channel of depth h, Rossby and Montgomery (1935) proposed the mixing length form

$$A_Z = \phi_m l^2 \left|\frac{\partial u}{\partial z}\right| = \alpha Z^2 \left(1 - \frac{Z}{h}\right)^2 \left|\frac{\partial u}{\partial z}\right| \phi_m \tag{7}$$

$$K_Z = \phi_s l^2 \left|\frac{\partial u}{\partial z}\right| = \alpha Z^2 \left(1 - \frac{Z}{h}\right)^2 \left|\frac{\partial u}{\partial z}\right| \phi_s \tag{8}$$

where Z=distance from the water surface; α=constant to be determined empirically; $|\partial u/\partial z|$=local value of vertical shear; l=mixing length; and ϕ variables are stability functions or damping functions which are parameterized in terms of gradient Richardson number. Park and Kuo (1993) proposed the following formula:

$$\phi_m = (1 + \beta \mathbf{R_i})^{-1/2} \tag{9}$$

$$\phi_s = (1 + \beta \mathbf{R_i})^{-3/2} \tag{10}$$

where the constants α and β are determined through model calibration and $\mathbf{R_i}$=local Richardson number.

The local (or gradient) Richardson number, a measure of water column stability, is defined as

$$\mathbf{R_i} = -\frac{g}{\rho}\left(\frac{\partial \rho}{\partial z}\right)\left(\frac{\partial u}{\partial z}\right)^{-2} \tag{11}$$

It is a dimensionless number representing the relative magnitude of the stabilizing force of the density stratification to the destabilizing influence of velocity shear. It may be also interpreted as the ratio of the buoyancy force to inertia force. The stability functions in Eqs. (7) and (8) account for the inhibition of the vertical exchanges of momentum and mass (salt) by a stable density structure.

Longitudinal Dispersion Coefficients

The longitudinal dispersion coefficients (A_x and K_x) are of the order of 10^5 of the vertical diffusion coefficients (Dyer 1973). Results of diffusion measurements in U.K. estuarine waters showed that K_x ranged from 10^4 to 10^6 cm^2/s (Talbot and Talbot 1974). Festa and Hansen (1976) studied the importance of the exact values of A_x and K_x. Varying the momentum exchange coefficient from $A_x = A_z$ to $A_x = 10^6 A_z$ caused negligible effect on the results of their tidal average model. The change, however, in mass exchange coefficient from $K_x = K_z$ to $K_x = 10^7 K_z$, did produce significant changes in their results.

The horizontal dispersion terms, despite their relative insignificance in the momentum balance, are retained in the model for the stability consideration. The present model used constant values for A_x and K_x and they are adjusted, within the range of 10^4 to 10^6 cm^2/s, through model calibration.

Model Calibration and Verification

For modeling purposes, the Tanshui River-Tahan Stream is treated as the mainstem of the river system, while the Hsintien Stream and Keelung River are treated as the first and second branches, respectively (Fig. 1). The model was supplied with data describing the geometry of the Tanshui River system. The geometry in the vertical two-dimensional model is represented by the width at each layer at the center of each grid cell. Field surveys in 1977 and 1995, made by the Taiwan Water Resources Agency, collected the cross-sectional profiles about every 0.5 km along the tidal portion of the river. These field data of cross-sectional profiles were used to schematize the estuary to prepare the geometric file for model input. The estuary was divided into 33, 14, and 43 segments and 33, 14, and 37 segments ($\Delta x = 1$ km) using the cross-sectional data collected in 1977 and 1995, respectively. The field data of cross-sectional profiles in 1977 were used because the earliest hydrographic data available for model calibration and verification were collected in 1977. The segment number in the Keelung River decreases because of the channel regulation in 1993.

The model with the 1995 geometric configuration has been calibrated with data collected in 1994 and 1995 (Hsu et al. 1999a,b). Manning's friction coefficient is the most important calibration parameter affecting the surface elevation, velocity, and flow. Since tidal flow constitutes the major portion of energy in the Tanshui River estuary, the Manning's coefficient was adjusted based on a comparison of the predicted tidal wave propagation with measured data. Both the spatially varying tidal range and phase were calibrated. Park and Kuo (1995) performed some sensitivity analyses with the original version of the model. They reported that the tidal range was very sensitive to the Manning's friction coefficient while the tidal phase was not. On the other hand, the tidal phase is very sensitive to the inclusion of shoals and shallow embayments as storage areas. Therefore it is essential to have accurate representation of the storage areas so that the model may be calibrated with respect to both tidal range and phase. The Tanshui River model includes the Kuan-Du wetland as a storage area. The calibrated model has the Manning's friction coefficient ranging from 0.026 to 0.032 for the Tanshui River-Tahan Stream, 0.015 for the Hsintien Stream, and from 0.016 to 0.023 for the Keelung River.

In most estuaries with significant river discharges, salinity may serve as an ideal natural tracer for calibration of mixing processes. Salinity distribution in an estuary is affected by the tidal

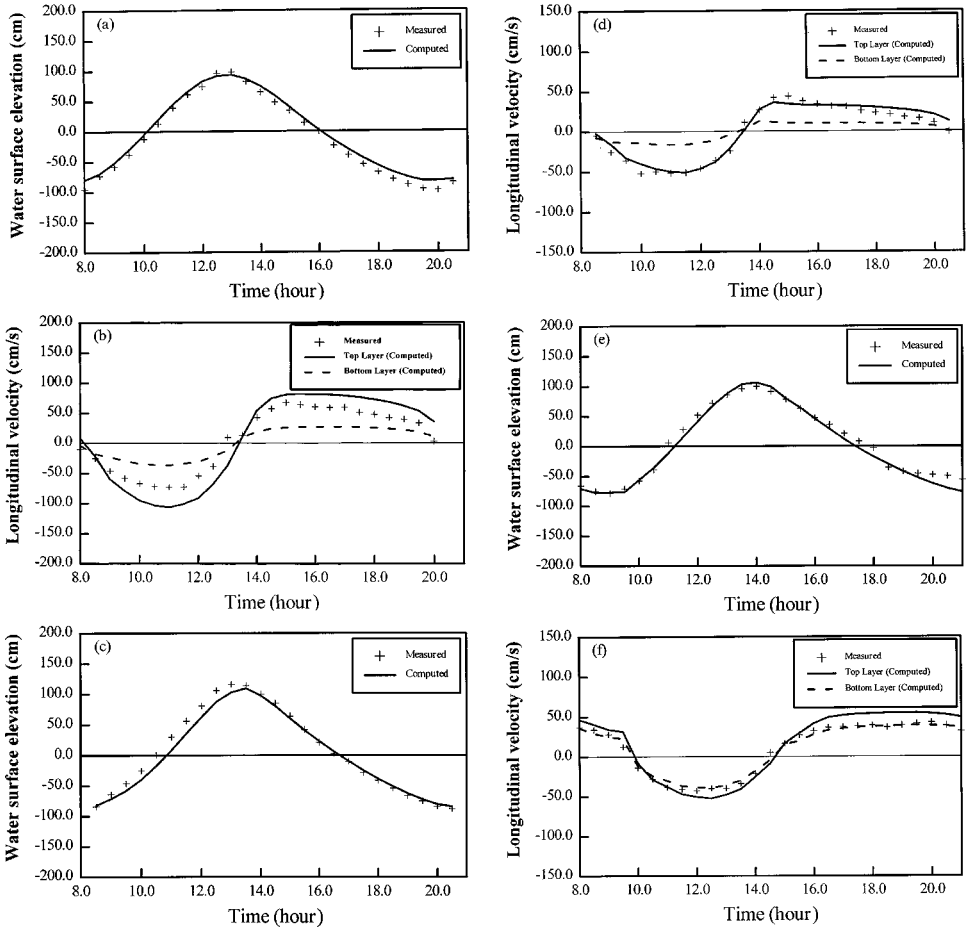

Fig. 5. Model reverification results: comparisons of measured and computed results on March 21, 1977: (a) Water surface elevation at Tu-Ti-Kung-Pi; (b) longitudinal velocity at Tu-Ti-Kung-Pi; (c) water surface elevation at Taipei Bridge; (d) longitudinal velocity at Taipei Bridge; (e) water surface elevation at Ta-Chih Bridge; and (f) longitudinal velocity at Ta-Chih Bridge

current, freshwater discharge, density circulation, as well as turbulent mixing processes. The two free constants in the expression of the turbulent diffusion coefficients are the major parameters requiring calibration. They were calibrated by matching the observed and computed salinity distributions. The results showed that the mean absolute differences and root-mean-square differences between the computed and hourly measured data were from 0.13 to 2.45 ppt at various stations (Hsu et al. 1999a). The overall model verification was achieved with comparison of salinity distributions at different times and the comparison of computed and observed Eulerian residual circulation. The successful simulation of the residual circulation indicated that the model accurately reproduced the baroclinic mode of motion, which is controlled by salinity (or density) distribution. The calibrated and verified constants for the turbulence model are $\alpha=0.0115$ and $\beta=0.75$. The calibrated and verified values of the longitudinal dispersion coefficients are $A_x=K_x=28\times10^5$ cm^2/s for the Tanshui River-Tahan Stream, $A_x=K_x=3.5\times10^5$ cm^2/s for the Hsintien Stream, and $A_x=K_x=5\times10^4$ cm^2/s for the Keelung River.

The objective of this study is to quantify the salinity changes between present river conditions and those prior to reservoir construction. Since the river geometry has changed substantially over the years, it is advisable to reverify or calibrate the model for conditions prior to reservoir construction. Unfortunately the earliest available hydrographic data for model verification were collected in 1977, and they are rather limited. The data consists of three 13-h time series of surface elevation and velocity at three stations each. No salinity data are available. Measurements were made at 30-min intervals over a full tidal cycle. Because of the shortage of field data for time series water surface elevations at the river mouth, a detailed calibration and verification such as that for the 1994 and 1995 conditions (Hsu et al. 1999a) was not possible. Thus the constants in the turbulence model obtained from the 1994 and 1995 calibration/verification were assumed valid. The same values of Manning's friction coefficient obtained from the 1994 and 1995 calibration/verification were also adopted for model verification with data of March 21, 1977. The model was run for 15 days with the observed 13-h surface elevation at the river mouth repeated for each tidal cycle as the open boundary condition. The measured daily river discharges over the corresponding 15-day period were used for the upstream boundary conditions. Fig. 5 shows comparisons between model results and field observations. The overall agreement between the model results and field data are satisfactory, considering the lack of proper boundary conditions. Table 1 presents the mean absolute differences and root-mean-square differences that measure the differences between the computed and measured time series data. They are comparable with those of model calibration/verification results using 1994 and 1995 data (Hsu et al. 1999a). Therefore it is concluded that the same set of calibrated coefficients are applicable to conditions prior to reservoir construction.

Table 1. Mean Absolute Differences and Root-Mean-Square Differences between Computed and Measured Time Series Water Surface Elevation and Longitudinal Velocity for Model Reverification of March 21, 1977

	Water surface elevation (cm)		Longitudinal velocity (cm/s) (cross-sectional average)	
Stations	Mean absolute difference	Root-mean-square difference	Mean absolute difference	Root-mean-square difference
Tu-Ti-Kung-Pi	8.35	9.28	7.77	10.61
Taipei Bridge	7.71	10.51	11.47	13.95
Ta-Chih Bridge	7.75	9.95	4.80	6.51

Model Application and Discussion

The reverified model was used to perform a series of model simulations to investigate salinity distributions before reservoir construction and under present conditions, respectively. The earliest available bathymetric data were collected in 1969, a time between the construction of the Shihman and Feitsui Reservoirs. These data (also presented in Fig. 3) were used to represent the geometric conditions prior to reservoir construction.

To simulate the salinity distributions pre- and post-reservoir construction, respectively, model simulations were conducted using nine constituent tides. They were extracted from a harmonic analysis using field data at the river mouth in 1995. The nine constituents were M_2 (12.42 h), S_2 (12 h), N_2 (12.9 h), K_1 (23.93 h), S_a (8,765.32 h), O_1 (25.82 h), K_2 (11.97 h), P_1 (24.07 h), and M_4 (6.21 h). Amplitudes and phases of the tidal constituents were specified to generate a time series of surface elevations as a downstream boundary condition for a 1-year (705 tidal cycle) model simulation. A high tide salinity of 35 ppt at the river mouth was used for model simulation. This is the typical value observed when river flow is below the long-term mean. The river discharges at the tidal limits of the three major tributaries, Tahan Stream, Hsintien Stream, and Keelung River, were specified as upstream boundary conditions. Table 2 lists the river discharges at upstream boundaries with mean flow (Q_m), Q_{50} flow (where Q_{50} is the flow that is equaled or exceeded for 50% of the time), and Q_{75} flow before and after reservoir construction.

Figs. 6 and 7 present the predicted salinity distributions before and after reservoir construction, respectively, under Q_{50} flow conditions. The computed salinities were averaged over 58 tidal cycles to smooth out the spring neap as well as the intratidal variations. The limits of salt intrusion after reservoir construction were farther up-river than that before reservoir construction in all three tributaries. This reflects the combined effects of the reduction in river discharges and the deepening and widening of the river. The limits of salt intrusion, represented by 1 ppt isohaline, are located 22.5 and 25 km from the river mouth in the Tahan Stream before and after reservoir construction, respectively. The surface salinity at the Keelung River mouth, where the Kuan-Du wetland is located, is of particular ecological significance. It controls the dominant vegetation types in the wetland. It increases from 12.5 to 15.8 ppt after reservoir construction. The patterns of salinity distributions under Q_m and Q_{75} flow conditions are similar to those under Q_{50}. They differ in the intrusion distance for specific isohaline. As the river flows decrease, the limits of salt intrusion move closer to the tidal limits and the difference between pre- and post-reservoir construction reduces. However, the salinity differences in the lower and middle parts of the estuary remain substantial. Tables 3 and 4 present the summary results of

Table 2. River Discharges at Upstream Boundaries before and after Reservoir Construction

Conditions	Upstream boundaries	Q_m (m^3/s) (mean flow)	Q_{50} (m^3/s) (medium flow)	Q_{75} (m^3/s) (low flow)
Before reservoir construction	Tahan Stream	69.82	29.65	18.10
	Hsintien Stream	82.83	44.43	20.43
	Keelung River	25.25	9.82	3.50
After reservoir construction	Tahan Stream	41.04	12.75	4.03
	Hsintien Stream	57.46	23.72	12.04
	Keelung River	25.25	9.82	3.50

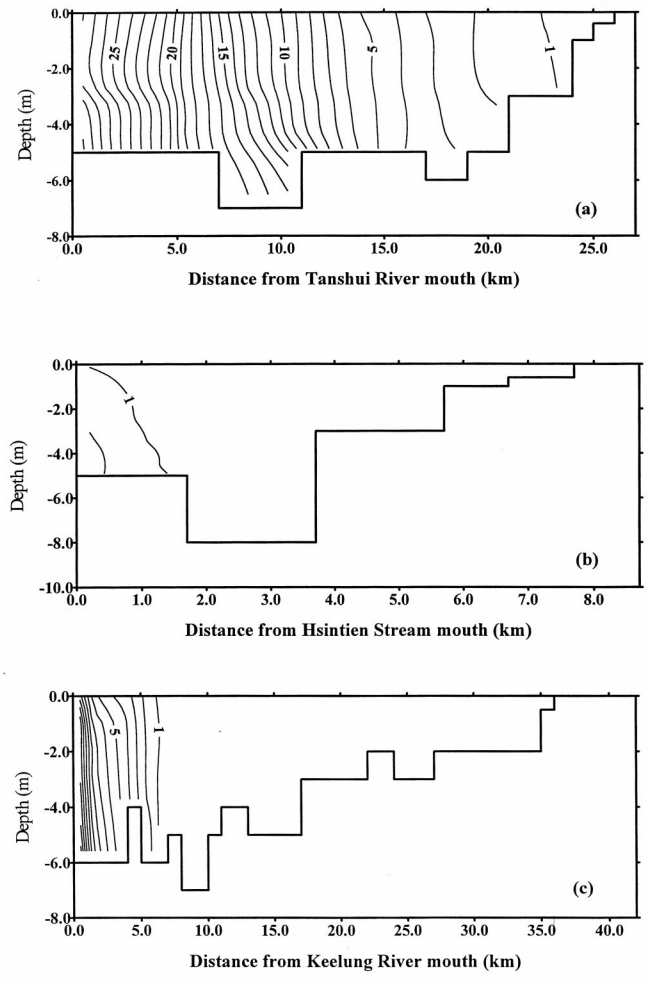

Fig. 6. Model prediction of salinity distributions before reservoir construction using Q_{50} flow condition: (a) Tanshui River-Tahan Stream; (b) Hsintien Stream; and (c) Keelung River. (The numbers on the contours refer to the salinity in parts per thousand.)

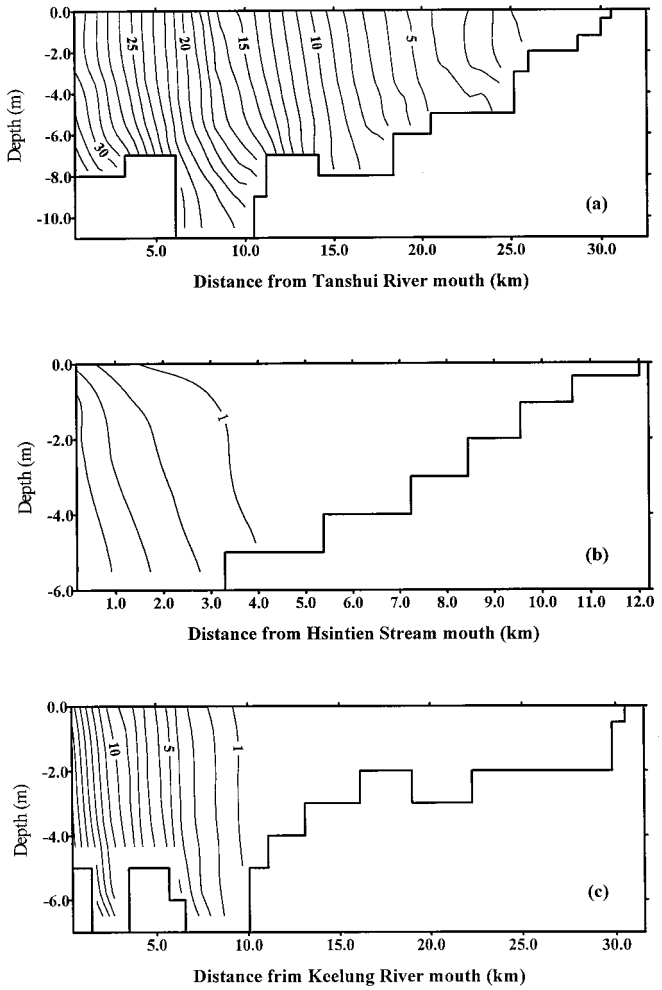

Fig. 7. Model prediction of salinity distributions after reservoir construction using Q_{50} flow condition: (a) Tanshui River-Tahan Stream; (b) Hsintien Stream; and (c) Keelung River. (The numbers on the contours refer to the salinity in parts per thousand.)

the salt intrusion limits in the Tahan Stream and the surface salinity in the river next to the Kuan-Du wetland under various river discharge conditions.

The above comparison of salinity distributions before and after the reservoir construction includes the combined effects of river discharge reduction and the enlargement of the river channel. To investigate each of the effects individually, two more model scenario runs were conducted. One run assumes the river geometry is unchanged while the mean river discharge is reduced after reservoir construction. The other run assumes no reservoir construction while the river geometry has changed from 1969 to 1995 conditions. Table 5 summarizes the results of the scenario runs,

Table 3. Limit of Salt Water Intrusion in the Tahan Stream under Various River Discharge Conditions

Limit of salt water intrusion (distance from Tanshui river mouth)	Before reservoir construction (km)	After reservoir construction (km)
Q_m	15	22
Q_{50}	22.5	25
Q_{75}	23.5	25.5

Table 4. Salinity near the Kuan-Du Wetland under Various River Discharge Conditions

Salinity near Kuan-Du wetland (surface layer at the Keelung River mouth)	Before reservoir construction (ppt)	After reservoir construction (ppt)
Q_m	5.8	10.3
Q_{50}	12.5	15.8
Q_{75}	18.1	19.1

together with those pre- and post-reservoir conditions. It shows that the change in river geometry has almost the same effect as the reduction in river discharge.

To examine the salinity change under the seasonally varying river discharge condition, another set of model simulations were conducted using average monthly flows before and after reservoir construction, respectively. Table 6 presents the average monthly flows at upstream boundaries of the three tributaries. It shows that the average monthly flows in the Tahan Stream and Hsintien Stream are significantly reduced after the reservoirs were constructed. The only exception is for the month of October in the Hsintien Stream. The flows in the Keelung River were unchanged, since no reservoir was constructed there. A nine-constituent tide and a high tide salinity of 35 ppt at the river mouth were used to force the downstream boundary conditions.

Fig. 8 presents the simulation results of the time series salinity variation in the surface layer at the Keelung River mouth near the Kuan-Du wetland. The salinity fluctuates in response to the variation of average monthly flows. However, the postreservoir condition has the salinity higher than the prereservoir condition at all times. The annual mean salinities before and after reservoir construction are 8.5 and 12.8 ppt, respectively. This suggests that the long-term salinity increases have the potential to favor the development of mangrove wetlands near the Keelung River mouth. In fact it has been suggested that salinity increase is the major culprit for the shift of vegetation types in the Kuan-Du wetland over the past 30 years (Wester 1988). It has also been reported that the

Table 5. Summary Results of Model Scenarios Using Mean Flow Condition

Conditions	Limit of salt water intrusion (distance from Tanshui River mouth) (km)	Salinity near Kuan-Du wetland (ppt)
1969 bathymetric configuration and mean discharge before reservoir construction	15	5.8
1995 bathymetric configuration and mean river discharge before reservoir construction	17.5	8.1
1969 bathymetric configuration and mean river discharge after reservoir construction	18	8.3
1995 bathymetric configuration and mean river discharge after reservoir construction	22	10.3

Table 6. Average Monthly Flows at the Upstream Boundaries of the Three Tributaries before and after Reservoir Construction

	Before reservoir construction			After reservoir construction		
Month	Tahan Stream[a]	Hsintien Stream[c]	Keelung River[e]	Tahan Stream[b]	Hsintien Stream[d]	Keelung River[e]
January	40.71	67.34	29.11	14.95	27.29	29.11
February	58.09	71.87	33.41	24.73	36.52	33.41
March	43.45	66.12	25.60	33.28	31.60	25.60
April	41.26	37.36	16.15	30.64	32.85	16.15
May	44.60	62.67	16.18	33.91	34.64	16.18
June	77.17	106.86	18.56	57.49	59.64	18.56
July	78.70	55.74	7.76	38.79	41.10	7.76
August	108.38	104.69	14.51	92.50	77.00	14.51
September	167.69	138.77	29.96	83.47	117.00	29.96
October	59.82	127.07	45.43	50.36	130.84	45.43
November	49.65	96.32	36.59	15.63	56.43	36.59
December	35.26	60.65	30.37	13.14	43.76	30.37

[a]Data collected from 1957 to 1964 before Shihman Reservoir was constructed.

[b]Data collected from 1965 to 1999 after Shihman Reservoir was constructed.

[c]Data collected from 1970 to 1986 before Feitsui Reservoir was constructed.

[d]Data collected from 1987 to 1999 after Feitsui Reservoir was constructed.

[e]Data collected from 1970 to 1999 since no reservoir was constructed in the Keelung River.

salinity increase might contribute to the reduction of green algae in the lower part of the estuary (Wu 2000).

The development of mangrove wetlands gradually replaced the less salt-tolerant vegetation. The resultant change in vegetation density would alter the capacity of the shallow storage area for the vertical two-dimensional model, but its effect is considered minimal and not included in model simulations. On the other hand, it is expected that the growth of mangroves would have a significant impact on the flow field in the event of flood. Liu et al. (2003) used a depth-averaged two-dimensional hydrodynamic model to investigate the effects of mangrove trees on flow resistance. They found that the flow pattern and resistance distribution were quite different over the mangrove area during high flow events. Therefore the increasing development of mangrove wetland would affect the resistance parameter used in a horizontal two-dimensional model.

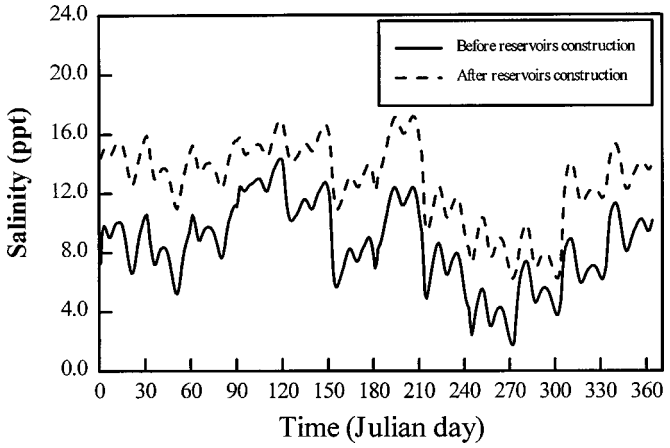

Fig. 8. Computed time series salinity in the surface layer near Kuan-Du wetland in the Keelung River

Conclusions

A vertical (laterally integrated) two-dimensional hydrodynamic and salt water intrusion numerical model was applied to the Tanshui River estuarine system. The model had previously been calibrated and verified with respect to the 1995 bathymertic configuration using observed time series water level, current, and salinity data of 1994 and 1995. The model was further reverified for the 1977 bathymetric configuration using limited data sets collected in 1977, the earliest intensive field survey conducted by the Taiwan Water Resources Agency. The model was then used to simulate the salinity distributions under different bathymetric configurations and for several scenarios of river flows before and after reservoir construction in the Tanshui River system.

The model simulations were conducted with three different constant river flow conditions, Q_m, Q_{50}, and Q_{75}, at upstream boundaries of the three tributaries for the periods before and after reservoir construction. A nine-constituent tide and a high tide salinity of 35 ppt at the river mouth were used as the downstream boundary conditions. The results show that the limit of salt intrusion moved farther up-river after the reservoirs were constructed. Substantial increases in salinity occurred throughout the estuary. Another set of model simulations was conducted using time varying river flows at upstream boundaries. Each simulation was performed for 1 year with average monthly flows for the periods before and after reservoir construction, respectively. The results show that the surface salinity near Kuan-Du wetland increased at all times of the year and the annual mean salinities before and after reservoir construction were 8.5 and 12.8 ppt, respectively.

It has been speculated that the long-term increase in salinity is the driving force altering the aquatic ecosystem structure in the lower reach of the river system and Kuan-Du mangrove swamp. The most noticeable change is the expansion of mangrove areas and the disappearing of freshwater marshes. Though there was no concrete evidence for the cause of the salinity increase, land subsidence has been suggested. This case study concludes that the combined effects of the freshwater withdrawal at the reservoirs and the enlargement of the river channel could be the causes of

the change. The two alternations of the river system contribute to roughly the same degree of salinity increases.

Acknowledgments

This study is supported by National Science Council, Taiwan, under Grant No. 90-2211-E-002-086. The writers thank the Taiwan Water Resources Agency for providing the prototype data. The writers also would like to express their appreciation to the three anonymous reviewers; through their comments this paper is substantially improved.

Notation

The following symbols are used in this paper:

A_x, A_z = turbulent viscosity in x and z directions, respectively;
B = river width;
B_η = width at free surface including side storage area;
g = gravitational acceleration;
H = total depth below mean sea level;
h = depth;
K_x, K_z = turbulent dispersion coefficient and diffusivity in x and z directions, respectively;
k = constant relating density to salinity ($=7.5 \times 10^{-4}$/ppt);
l = mixing length;
p = pressure;
q = lateral inflow per unit river length;
q_p = lateral inflow per unit lateral area;
$\mathbf{R_i}$ = gradient Richardson number;
S_0 = source and sink of salt due to exchange with side storage area;
s = laterally averaged salinity;
t = time;
u = laterally averaged velocity in x direction;
w = laterally averaged velocity in z direction;
x = distance seaward along river axis;
Z = distance from the water surface;
z = distance upward in vertical direction;
α, β = constants;
$|\partial u/\partial z|$ = local value of vertical shear;
η = position of free surface above mean sea level;
ρ = water density;
ϕ_m = stability function for momentum; and
ϕ_s = stability function for mass.

References

Blumberg, A. F. (1977). "Numerical model of estuarine circulation." *J. Hydraul. Div., Am. Soc. Civ. Eng.*, 103(3), 295–310.

Blumberg, A. F. (1986). "Turbulent mixing processes in lakes, reservoirs, and impoundments." *Physics-based modeling of lakes, reservoir, and impoundments*, W. G. Gray, ed., ASCE, New York, 79–104.

Blumberg, A. F., Khan, L. A., and John, J. P. St. (1999). "Three-dimensional hydrodynamic model of New York harbor region." *J. Hydraul. Eng.*, 125(8), 799–816.

Casulli, V., and Cheng, R. T. (1992). "Semi-implicit finite difference methods for the three-dimensional shallow water flow." *Int. J. Numer. Methods Fluids*, 15, 629–648.

Dyer, K. R. (1973). *Estuaries: A physical introduction*, Wiley, New York.

Festa, J. F., and Hansen, D. V. (1976). "A two-dimensional numerical model of estuarine circulation: the effects of altering depth and river discharge." *Estuarine Coastal Mar. Sci.*, 4, 309–323.

Hall, R. W., and Chapman, R. S. (1985). "Two-dimensional QUICKEST; solution of the depth-average transport-dispersion equation." *Technical Rep. EL-85-3*, US Army Corps of Engineers, Vicksburg, Miss.

Hsu, M. H., Kuo, A. Y., Kuo, J. T., and Liu, W. C. (1996). "Study of tidal characteristics, estuarine circulation and salinity distribution in Tanshui River system (I)." *Technical Rep. No. 239*, Hydrotech Research Institute, National Taiwan University, Taipei, Taiwan (in Chinese).

Hsu, M. H., Kuo, A. Y., Kuo, J. T., and Liu, W. C. (1997). "Study of tidal characteristics, estuarine circulation and salinity distribution in Tanshui River system (II)." *Technical Rep. No. 273*, Hydrotech Research Institute, National Taiwan University, Taipei, Taiwan (in Chinese).

Hsu, M. H., Kuo, A. Y., Kuo, J. T., and Liu, W. C. (1999a). "Procedure to calibrate and verify numerical models of estuarine hydrodynamics." *J. Hydraul. Eng.*, 125(2), 166–182.

Hsu, M. H., Kuo, A. Y., Liu, W. C., and Kuo, J. T. (1999b). "Numerical simulation of circulation and salinity distribution in the Tanshui estuary." *Proc. Natl. Sci. Counc., Repub. China, Part A: Phys. Sci. Eng.*, 23(2), 259–273.

Johnson, B. H., Kim, K. W., Heath, R. E., Hsieh, B. B., and Butler, H. L. (1993). "Validation of 3-D hydrodynamic model of Chesapeake Bay." *J. Hydraul. Eng.*, 119(1), 2–20.

Kjerfve, B. (1976). "The Santee-Cooper: A study of estuarine manipulations." *Estuarine processes*, Vol. 1 M. Wiley, ed., Academic, Orlando, Fla., 44–56.

Kjerfve, B., and Greer, J. E. (1978). "Hydrography of the Santee River during moderate discharge conditions." *Estuaries*, 1, 111–119.

Kuo, A. Y., and Liu, W. C. (2001). "Investigation of hydrodynamic characteristics in the Tanshui River estuarine system." *2001 Agricultural Engineering Annual Conference*, Dept. of Agricultrual Engineering, National Taiwan Univ., Taipai, Taiwan, 1–13 (in Chinese).

Lai, Y. G., Weber, L. J., and Patel, V. C. (2003). "Nonhydrostatic three-dimensional model for hydraulic flow simulation. I: Formulation and verification." *J. Hydraul. Eng.*, 129(3), 196–205.

Leonard, B. P., Vachtsevanos, G. J., and Abood, K. A. (1978). "Unsteady-state, two-dimensional salinity intrusion model for an estuary." *Applied numerical modelling*, C. Brebbia, ed., Pen Tech. Press, 113–123.

Liu, W. C., Hsu, M. H., and Wang, C. F. (2003). "Modeling of flow resistance in mangrove swamp at mouth of tidal Keelung River, Taiwan." *J. Waterw., Port, Coastal, Ocean Eng.*, 129(2), 86–92.

McAlice, B. J., and Jaeger, Jr., G. B. (1983). "Circulation changes in the Sheepscot River estuary, Maine, following removal of a causeway." *Estuaries*, 6, 190–199.

Park, K., and Kuo, A. Y. (1993). "A vertical two-dimensional model of estuarine hydrodynamics and water quality." *Special Report of Applied Marine Science Sci. and Ocean Eng. No. 321*, Virginia Institute of Marine Science, Gloucester Point, Va.

Park, K., and Kuo, A. Y. (1995). "A framework for coupling shoals and shallow embayments with main channels in numerical modeling of coastal plain estuaries." *Estuaries*, 18(2), 341–350.

Pritchard, D. W. (1954). "A study of salt balance in a coastal plain estuary." *J. Mar. Res.*, 13(1), 133–144.

Pritchard, D. W. (1956). "The dynamic structure of a coastal plain estuary." *J. Mar. Res.*, 15(1), 33–42.

Roache, P. J. (1972). *Computational fluid dynamics*, Hermosa, Socorro, N.M.

Rossby, C. G., and Montgomery, R. B. (1935). "The layer of frictional influence in wind and ocean currents." *Physical oceanography and meteorology*.

Talbot, J. W., and Talbot, G. A. (1974). "Diffusion in shallow seas and in English coastal and estuarine waters." *Rapp. P.-V. Reun.-Cons. Int. Explor. Mer*, 167, 93–110.

Wang, I. Z. (1999). "An ecological study of estuarine wetlands-A case study of the changing vegetations of Kuan-Du mangrove swamp." Masters thesis, National Taiwan University, Taipei, Taiwan (in Chinese).

Wang, J. D., Blumberg, A. F., Bulter, H. L., and Hamilton, P. (1990). ''Transport prediction in partially stratified tidal water.'' *J. Hydraul. Eng.*, 116(3), 380–396.

Wang, L. L., Mysak, A., and Ingram, R. G. (1994). ''A 3-D numerical simulation of Hudson Bay summer circulation.'' *J. Phys. Oceanogr.*, 24, 2496–2514.

Wester, L. (1988). ''Vegetation change in Kuan-Du marsh, Taiwan 1978–1985.'' *Detailed planning of Kuan-Du National Park*, Taipei City Government, Taipei, 415–426.

Wu, J. T. (2000). ''Establishment of ecological monitoring system in Tanshui River estuary.'' Report to Institute of Academic Sinica, Taipei, Taiwan (in Chinese).